

RESEARCH ARTICLE | FEBRUARY 06 2026

Dynamic magnetoelectric effect in multiferroic DyCrO₄ FREE

Xiaonan Yuan  ; Yingjie He  ; Deshun Hong   ; Xudong Shen  ; Youwen Long  ; Young Sun  



Appl. Phys. Lett. 128, 052902 (2026)

<https://doi.org/10.1063/5.0315219>



Articles You May Be Interested In

Engineering DyCrO₃ ceramics toward room-temperature high-κ dielectric applications

J. Appl. Phys. (October 2023)

High-pressure Raman scattering study on zircon- to scheelite-type structural phase transitions of R CrO₄


J. Appl. Phys. (May 2008)

Suppression of magnetoelectric effects in DyCrO₄ by chemical doping

Appl. Phys. Lett. (February 2020)

AIP Advances

Why Publish With Us?



21DAYS
average time
to 1st decision



OVER 4 MILLION
views in the last year



INCLUSIVE
scope

[Learn More](#)



Dynamic magnetoelectric effect in multiferroic DyCrO₄

Cite as: Appl. Phys. Lett. **128**, 052902 (2026); doi: [10.1063/5.0315219](https://doi.org/10.1063/5.0315219)

Submitted: 4 December 2025 · Accepted: 21 January 2026 ·

Published Online: 6 February 2026



View Online



Export Citation



CrossMark

Xiaonan Yuan,¹ Yingjie He,¹ Deshun Hong,^{1,a)} Xudong Shen,^{2,3} Youwen Long,⁴ and Young Sun^{1,a)}

AFFILIATIONS

¹Department of Applied Physics and Center of Quantum Materials and Devices, Chongqing University, Chongqing 401331, China

²Spallation Neutron Source Science Center, Dongguan 523803, China

³Institute of High Energy Physics, Chinese Academy of Science, Beijing 100049, China

⁴Beijing National Laboratory for Condensed Matter Physics, Institute of Physics, Chinese Academy of Sciences, Beijing 100190, China

^{a)}Authors to whom correspondence should be addressed: dhong@cqu.edu.cn and youngsun@cqu.edu.cn

ABSTRACT

The dynamic magnetoelectric (ME) effect of the scheelite-type DyCrO₄ has been investigated by measurements of the temperature and magnetic field dependence of the dynamic magnetoelectric coefficient ($\alpha_E = dE/dH$). A high dynamic ME coefficient α_E is obtained in the multiferroic phase after a poling process under both electric and magnetic fields. The maximum of α_E appears at the critical field of a metamagnetic transition where spin fluctuation becomes the most significant. The dynamic ME effect for $H \perp E$ is much stronger than that for $H \parallel E$, consistent with the spin current model. Moreover, the sign of α_E is reversed when the direction of electric polarization is reversed by a negative electric field. Therefore, the state of α_E can be used to store information in single-phase multiferroics.

Published under an exclusive license by AIP Publishing. <https://doi.org/10.1063/5.0315219>

The magnetoelectric (ME) effects are characterized by the appearance of electric polarization P (magnetization M) under the application of a magnetic field H (electric field E), which has attracted wide attention in terms of both fundamental science and potential applications.^{1–3} In the past decades, significant research efforts have been devoted to discovering ME materials and understanding the underlying physics of ME phenomena. Especially, multiferroic materials stand out as the mainstream in the study of the ME effects.

Multiferroicity refers to the coexistence of two or more ferroic properties: ferroelectricity, ferromagnetism, and ferroelasticity.^{4,5} The type-II multiferroics, where ferroelectricity is induced by specific magnetic orders, are the most promising materials for achieving larger ME effects.⁵ For example, transition metal oxides with spiral magnetic structures such as manganites,^{6–9} and hexaferrites^{10–12} have been found to exhibit significant ME effects. While the static ME effect and the direct ME coefficient $\alpha_D = dP/dH$ have been intensively investigated for single-phase multiferroics, the dynamic ME effect and the ME voltage coefficient $\alpha_E = dE/dH$ remain less studied in single-phase ME materials. The measurement and calculation of α_D are usually complicated because the detection of ΔP is not straightforward in experiments but determined by integrating the released current with time. In contrast, α_E can be directly measured by a dynamic method in which an ac magnetic field induces an ac voltage on the sample due to

the ME effect.^{13,14} As a matter of fact, the dynamic ME voltage coefficient α_E has been generally measured in multiferroic composites, but little attention has been paid to that in single-phase multiferroics.

The chromates $R\text{CrO}_4$ (R is a rare earth element) family has drawn considerable interest in recent years for their unusual physical properties.^{15–26} These compounds crystallize in a tetragonal zircon-type structure with the space group $I4_1/amd$ under ambient conditions.^{15–19} Nevertheless, the structure of the $R\text{CrO}_4$ family is sensitive to external pressures.^{20–22} Under high pressure, the zircon-type $R\text{CrO}_4$ compounds, such as DyCrO₄, undergo an irreversible structural phase transition to a scheelite-type phase with space group $I4_1/a$.²² This transition is characterized by a substantial volume collapse of approximately 10%. Notably, the magnetic properties of these $R\text{CrO}_4$ compounds are highly dependent on their crystalline structure.^{23–25} The zircon-type DyCrO₄ exhibits long-range ferromagnetic ordering below ~ 23 K, whereas the scheelite-type DyCrO₄ displays antiferromagnetic (AFM) behavior. DyCrO₄ is an ideal model system for studying $3d$ - $4f$ electronic interactions as it contains two distinct magnetic ions, Dy³⁺ and Cr⁵⁺, which give rise to competing spin interactions.²³ Furthermore, both the zircon- and scheelite-type polymorphs of DyCrO₄ exhibit remarkable physical properties, such as metamagnetic transitions,²⁴ and magnetic field-induced sign change of thermal expansion.²⁶ Moreover, in the scheelite-type DyCrO₄, the magnetic

point group $2'/m$ allows for a non-zero linear ME tensor, indicative of a linear ME effect.

Although spin-induced ferroelectricity and a large linear ME effect were experimentally confirmed in the scheelite-type DyCrO_4 ,²⁴ its dynamic ME effect has not been reported yet. In this Letter, we present a systematic investigation on the temperature and magnetic field dependence of the dynamic ME coefficient (α_E) of the scheelite-type DyCrO_4 .

Polycrystalline zircon-type DyCrO_4 samples were synthesized from stoichiometric mixtures of $\text{Dy}(\text{NO}_3)_3 \cdot 6\text{H}_2\text{O}$ and $\text{Cr}(\text{NO}_3)_3 \cdot 9\text{H}_2\text{O}$. The detailed synthesis procedure has been described in previous reports.²⁴ Subsequently, black scheelite-type DyCrO_4 was obtained from a green zircon-type DyCrO_4 precursor by treatment under 3.0 GPa and 850 K for 15 min using a cubic anvil-type high-pressure apparatus. The magnetic properties were measured by using a Magnetic Property Measurement System (MPMS-3, Quantum Design). The specific heat (C_p), dielectric permittivity ϵ_r and the dynamic ME coefficient α_E were measured in a Physical Property Measurement System (PPMS-9 T, Quantum Design). The dielectric permittivity was measured using an LCR meter (Agilent E4980A). The linear ME voltage coefficient $\alpha_E = dE/dH$ was measured by the dynamic method using a home-made probe.^{13,14} An ac current supplied to a solenoid generates a small ac magnetic field (H_{ac}) at a frequency of 997 Hz, and the induced ac ME voltage on the sample, $V_{ac} = V_x + iV_y$ (where V_x and V_y represent the in-phase and out-of-phase signals, respectively) was detected by a lock-in amplifier. The dynamic ME coefficient α_E was calculated as $\alpha_E = V_x/(H_{ac}d)$, where d is the distance between the up

and down electrodes. Prior to the measurements of α_E , a pre-poling process was performed to drive the sample into the ferroelectric state. A poling electric field and magnetic field were simultaneously applied at 50 K, then the sample was cooled from 50 to 2 K at a rate of 2 K/min. Upon stabilizing at 2 K, the poling electric field was removed and the sample was short-circuited for 30 min. Subsequently, α_E was measured during warming from 2 to 50 K at a rate of 2 K/min under zero or applied magnetic fields.

Figure 1(a) shows the temperature dependence of magnetic susceptibility measured in $H = 100$ Oe after zero-field cooling and specific heat (C_p) under zero magnetic field between 10 and 50 K. Both measurements indicate an AFM phase transition at $T_N \sim 24$ K, consistent with previous reports.^{24,26} At $T = 50$ K (above T_N), the magnetization shows a nearly linear dependence on the magnetic field in accordance with the paramagnetic phase. At $T = 2$ K, the magnetization exhibits nonlinearity, and a metamagnetic transition occurs around $\mu_0 H \approx 3$ T. At 10 K, the critical field for the metamagnetic transition shifts to approximately 3.1 T, in agreement with the phase diagram reported in previous studies. Neutron diffraction experiments reveal that DyCrO_4 adopts a collinear AFM structure at low temperatures, as illustrated in Fig. 1(c).²⁴ When the applied magnetic field exceeds the critical value, the magnetic configuration transforms into the canted AFM structure illustrated in Fig. 1(d).²⁴ The observed spin canting may arise from the combined contributions of both Dy^{3+} and Cr^{5+} spin sublattices, or it may be predominantly attributed to the Dy^{3+} sublattice alone.

The temperature dependence of the relative dielectric permittivity ϵ_r of the scheelite-type DyCrO_4 is presented in Figs. 2(a)–2(d). While

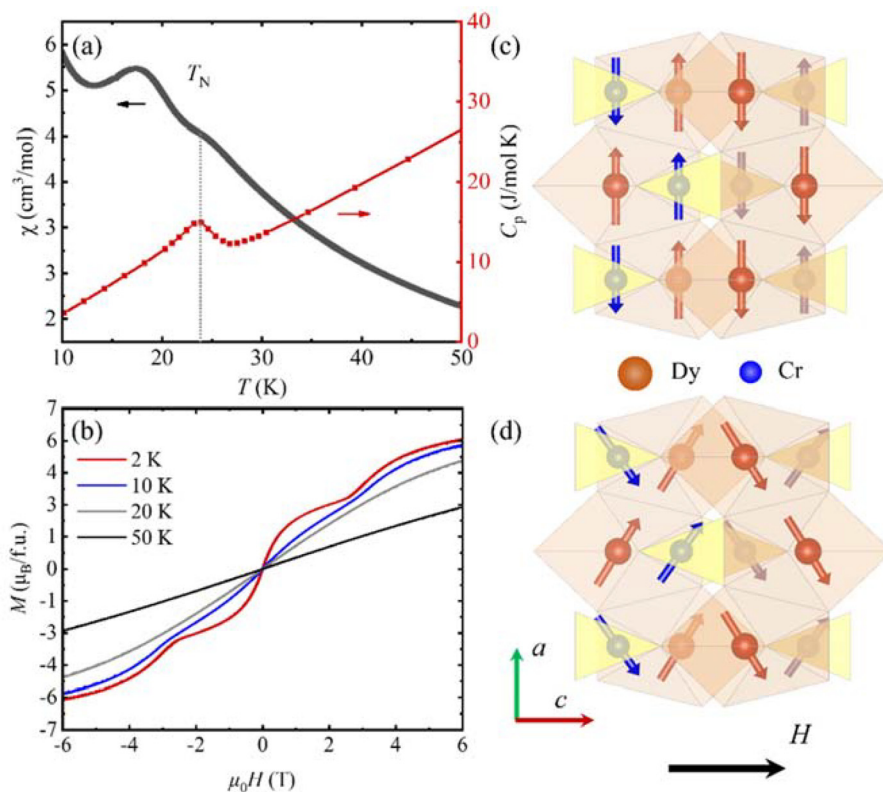


FIG. 1. (a) Temperature dependence of magnetic susceptibility and heat capacity of the scheelite-type DyCrO_4 . The dashed vertical line indicates the antiferromagnetic transition temperature T_N . (b) Isothermal magnetization at selected temperatures. Crystal and antiferromagnetic spin structures of the scheelite-type DyCrO_4 in (c) zero field and (d) high fields.

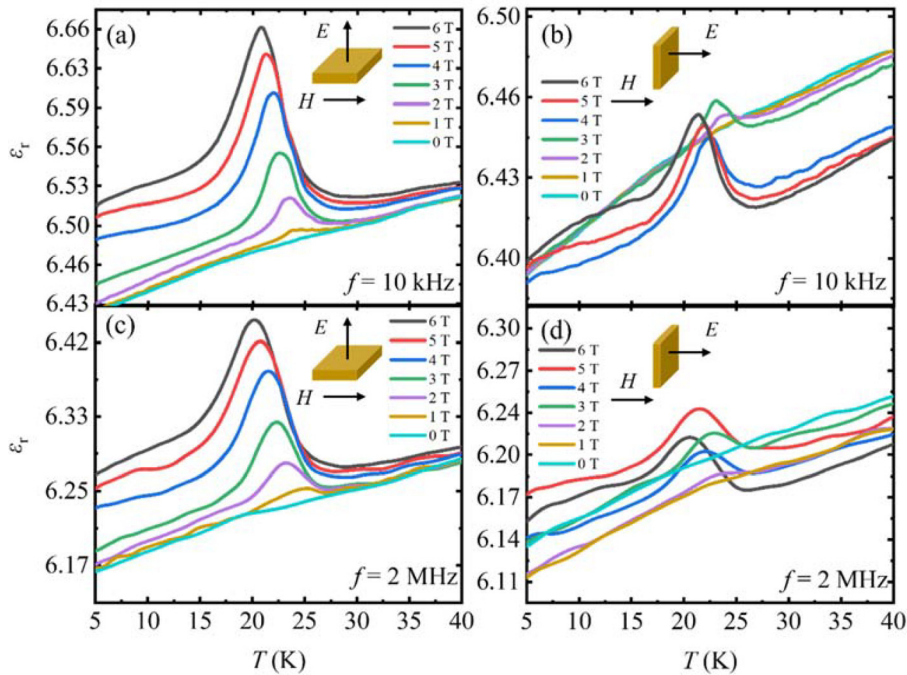


FIG. 2. (a) and (c) Temperature dependence of the dielectric permittivity ϵ_r at 10 kHz and 2 MHz under magnetic fields applied perpendicular to the electric field. (b) and (d) Temperature dependence of ϵ_r at 10 kHz and 2 MHz under magnetic fields applied parallel to the electric field.

no dielectric anomaly is observed in zero magnetic field, a clear dielectric peak emerges near 24 K upon the application of a magnetic field. It is worth noting that for both $H \perp E$ and $H \parallel E$ configurations, the dielectric peak shifts progressively toward lower temperatures. However, a pronounced enhancement of the peak with increasing magnetic field is observed in the $H \perp E$ configuration, whereas this effect is considerably less evident in the $H \parallel E$ configuration.

This dielectric behavior is independent of frequency. The magnetic field-induced dielectric peak is strong evidence of spin-induced ferroelectricity in the scheelite-type DyCrO_4 .²⁴ The collinear AFM phase belongs to the magnetic point group $2'/m$. Under an applied magnetic field, this symmetry is lowered from the initial non-polar group $2'/m$ to the polar group m , thereby giving rise to a spontaneous ferroelectric polarization. The symmetry of the induced magnetic point group permits non-zero ME tensor components, such as α_{13} (α_{31}) and α_{23} (α_{32}) in the following equation:

$$\alpha_E = \begin{pmatrix} 0 & 0 & \alpha_{13} \\ 0 & 0 & \alpha_{23} \\ \alpha_{31} & \alpha_{32} & 0 \end{pmatrix}. \quad (1)$$

This indicates that an electric polarization P can be generated perpendicular to the direction of the applied magnetic field H . A comparison of the dielectric response under different magnetic field orientations reveals the mechanism of spin-induced ferroelectricity. Specifically, the response for $H \parallel E$ [Figs. 2(b) and 2(d)] is substantially weaker than that for $H \perp E$ [Figs. 2(a) and 2(c)], which suggests that the spin-induced electric polarization is mainly perpendicular to applied magnetic fields, in accordance with the spin current model in type-II multiferroics.²⁷

The dynamic ME coefficient α_E as a function of temperature is shown in Fig. 3(a). After the pre-poling process under both an

electric field ($E_{\text{pol}} = 0.6$ MV/cm) and a dc magnetic field ($\mu_0 H = 0, 1, 2, 3, 4, 6, 9$ T), α_E was measured with increasing temperature. In the case of zero magnetic field, α_E remains negligible at all temperatures. When a 1 T magnetic field is applied in plane ($H \perp E$), α_E becomes significant below $T_N \sim 24$ K. It is noteworthy that a negative peak in the ME coefficient emerges at high temperatures when the applied magnetic field exceeds 2 T. This negative peak shifts toward lower temperatures with increasing magnetic field, similar to the behavior of the dielectric peak near T_N . Previous studies have suggested that strong spin fluctuations in the vicinity of magnetic phase transitions would lead to the emergence of a maximum in the dynamic ME coefficient.^{13,14} Therefore, the negative peak in the vicinity of T_N is likely due to strong spin fluctuation and spin-induced electric polarization in DyCrO_4 .

At low temperatures, α_E exhibits a distinct plateau-like region. The amplitude of α_E increases with increasing magnetic field until 3 T because spin-induced electric polarization grows with magnetic field.²⁴ Then, the amplitude of α_E decays with further increasing magnetic field and becomes negligible for $\mu_0 H \geq 6$ T as spin-induced ferroelectricity is weakened under higher magnetic fields. This result suggests that a significant dynamic ME effect appears in the spin-induced multiferroic phase, and its amplitude is dependent on the strength of ferroelectricity. The close correlation between the amplitude of α_E and electric polarization is more evident in Fig. 3(b). When the poling electric field increases under a constant $\mu_0 H = 3$ T, the amplitude of α_E grows from $450 \mu\text{V}/\text{cm Oe}$ for $E_{\text{pol}} = 0.6$ MV/m to $770 \mu\text{V}/\text{cm Oe}$ for $E_{\text{pol}} = 1.06$ MV/m. Since a higher poling electric field would induce a larger net electric polarization, the enhancement of α_E under a higher poling electric field reveals a proportion between α_E and electric polarization.

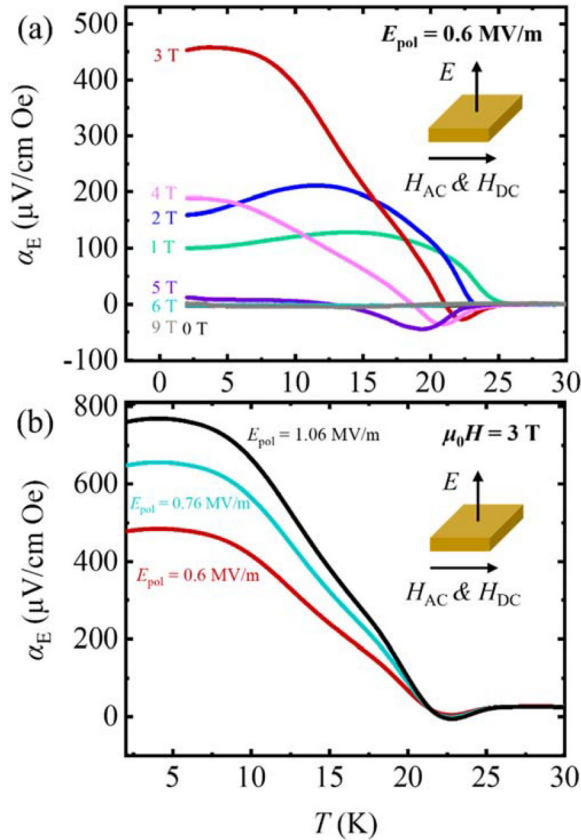


FIG. 3. (a) Temperature dependence of the dynamic ME coefficient α_E measured with increasing temperature under different magnetic fields ($H \perp E$) after a poling process. (b) Temperature dependence of α_E measured with increasing temperature under a fixed magnetic field of $\mu_0 H = 3$ T ($H \perp E$) after a poling process with different poling electric fields.

We also measured the dynamic ME coefficient α_E under reversed poling electric fields. As shown in Figs. 4(a) and 4(b), the sign of α_E becomes negative after a negative electric field poling. This result suggests that the value of α_E depends on not only the amplitude but also the direction of electric polarization. This feature enables a nondestructive reading of ferroelectric memory because the direction of electric polarization in the ferroelectric memory cell can be detected by measuring the sign of α_E . Moreover, the dynamic ME effect for $H \perp E$ is much stronger than that for $H \parallel E$. As seen in Figs. 4(a) and 4(b), the amplitude of α_E for $H \perp E$ is about five times higher than that for $H \parallel E$ under the same poling condition. This behavior is consistent with the mechanism of spin-induced electric polarization in DyCrO_4 , where the spin-induced electric polarization is perpendicular to the spin plane.²⁴

To elucidate why the dynamic ME effect is the most significant around 3 T, we measured the magnetic field dependence of α_E at fixed temperatures (2 and 10 K) after the field-poling process. As shown in Figs. 5(a)–5(c) at 2 K, α_E is quite small at high magnetic fields, then it grows with decreasing magnetic field and reaches the maximum at 3 T. The sharp peaks of α_E at ± 3 T are consistent with

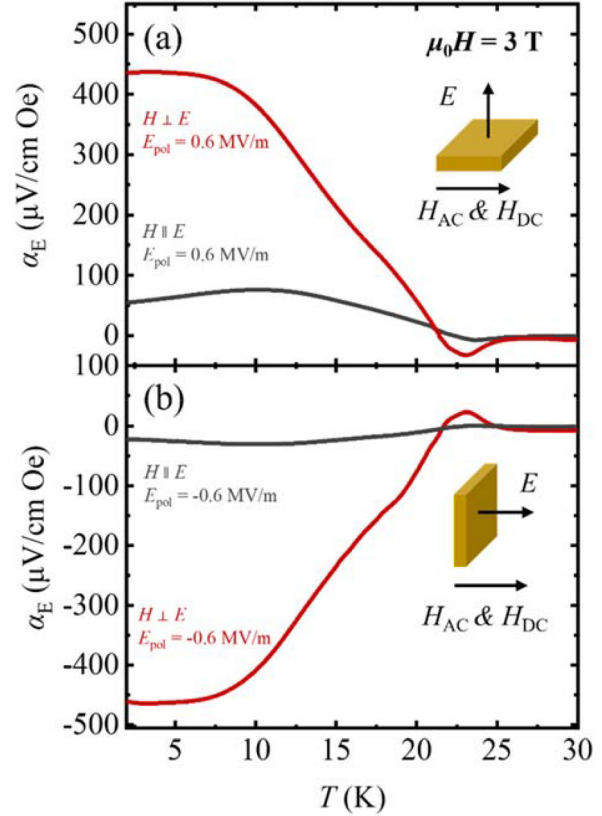


FIG. 4. Temperature dependence of the dynamic ME coefficient α_E measured with increasing temperature under a fixed magnetic field of $\mu_0 H = 3$ T ($H \perp E$ or $H \parallel E$) after a poling process with (a) a positive poling electric field and (b) a negative poling electric field. The sign of α_E is reversed when the electric polarization is reversed. The amplitude of α_E for $H \perp E$ is much higher than that for $H \parallel E$.

the M - H curve, where the metamagnetic transition occurs at ± 3 T. When the poling electric field is negative, the sign of α_E is reversed and the peaks become dips [Fig. 5(b)]. Similar behaviors are observed at 10 K, as shown in Figs. 5(d)–5(f). These results confirm that the dynamic ME effect is maximum at magnetic phase transitions, where spin fluctuation is the most significant. We note that the magnetic field dependence of the dynamic ME coefficient is identical to the behavior of the static ME coefficient obtained by dP/dH in a previous study.²⁴

In summary, we have investigated the dynamic ME effect in the scheelite-type DyCrO_4 . A high dynamic ME coefficient α_E is obtained in the multiferroic phase after a poling process under both electric and magnetic fields. The maximum of α_E appears at 3 T, where a metamagnetic transition occurs. Moreover, the dynamic ME effect for $H \perp E$ is much stronger than that for $H \parallel E$. These results suggest that a significant dynamic ME effect can be achieved at the phase boundaries in spin-induced type-II multiferroics. The sign of α_E depends on the direction of electric polarization controlled by the electric field. Therefore, the state of α_E can be used to store information in single-phase multiferroics.

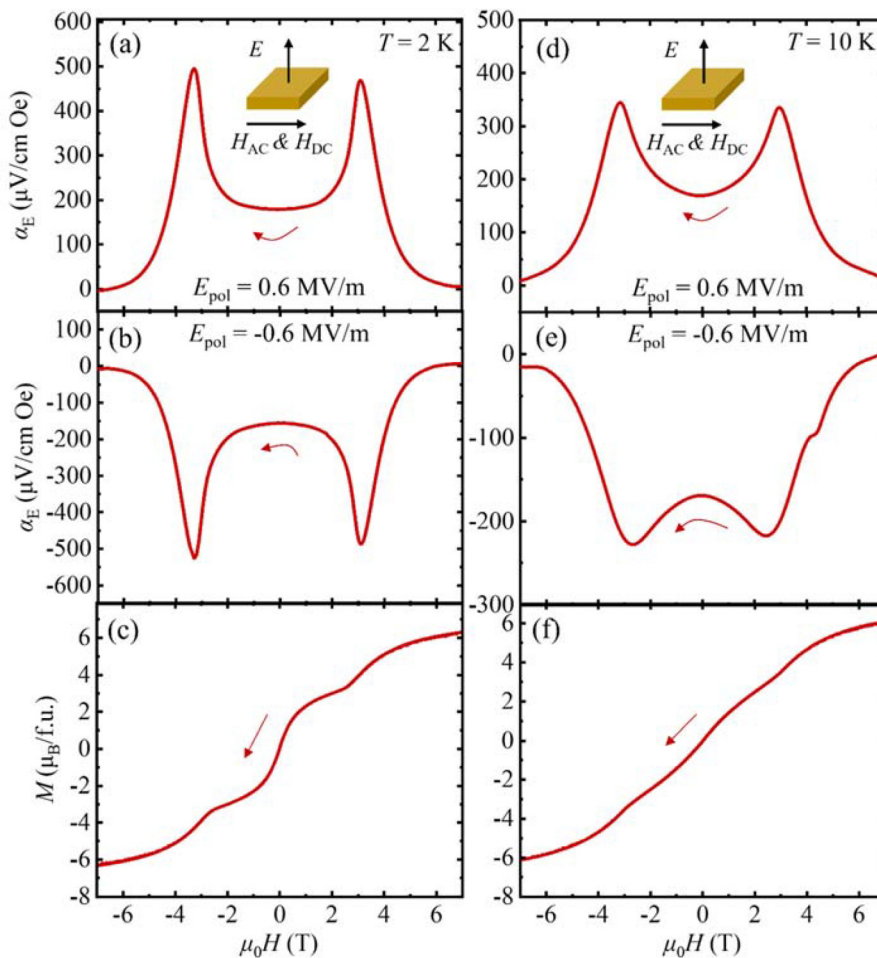


FIG. 5. Comparison between the field dependence of α_E and magnetization at (a)–(c) 2 K and (d)–(f) 10 K. After a poling process under $\mu_0 H = 3$ T and $E_{\text{pol}} = \pm 0.6$ MV/m, α_E was measured from 6 T to -6 T. The sharp peaks in α_E appear at the metamagnetic transition fields.

This paper was supported by the National Key Research and Development Program of China (Grant No. 2021YFA1400303) and the National Natural Science Foundation of China (Grant Nos. 12227806, 12425403, and 12261131499). Y.S. acknowledges the Fundamental Research Funds for the Central Universities (Project No. 2025CDJ-IAISZD-005).

AUTHOR DECLARATIONS

Conflict of Interest

The authors have no conflicts to disclose.

Author Contributions

Xiaonan Yuan: Data curation (lead); Formal analysis (equal); Investigation (equal); Methodology (equal); Writing – original draft (lead). **Yingjie He:** Data curation (equal); Methodology (lead). **Deshun Hong:** Formal analysis (equal); Investigation (equal); Methodology (equal); Supervision (equal). **Xudong Shen:** Resources (equal). **Youwen Long:** Resources (equal); Writing – review & editing (supporting). **Young Sun:** Conceptualization (lead); Formal analysis (equal); Funding acquisition (lead); Investigation (lead); Supervision (lead); Writing – review & editing (lead).

DATA AVAILABILITY

The data that support the findings of this study are available from the corresponding authors upon reasonable request.

REFERENCES

- ¹N. A. Spaldin and M. Fiebig, “The renaissance of magnetoelectric multiferroics,” *Science* **309**, 391 (2005).
- ²M. Fiebig, “Revival of the magnetoelectric effect,” *J. Phys. D: Appl. Phys.* **38**, R123 (2005).
- ³F. Matsukura, Y. Tokura, and H. Ohno, “Control of magnetism by electric fields,” *Nat. Nanotechnol.* **10**, 209 (2015).
- ⁴H. Schmid, “Multi-ferroic magnetoelectrics,” *Ferroelectrics* **162**, 317 (1994).
- ⁵D. I. J. P. Khomskii, “Classifying multiferroics: Mechanisms and effects,” *Physics* **2**, 20 (2009).
- ⁶T. Kimura, T. Goto, H. Shintani, K. Ishizaka, T. Arima, and Y. Tokura, “Magnetic control of ferroelectric polarization,” *Nature* **426**, 55 (2003).
- ⁷T. Aoyama, K. Yamauchi, A. Iyama, S. Picozzi, K. Shimizu, and T. Kimura, “Giant spin-driven ferroelectric polarization in TbMnO₃ under high pressure,” *Nat. Commun.* **5**, 4927 (2014).
- ⁸T. Aoyama, A. Iyama, K. Shimizu, and T. Kimura, “Multiferroicity in orthorhombic RMnO₃ (R = Dy, Tb, and Gd) under high pressure,” *Phys. Rev. B* **91**, 081107 (2015).
- ⁹T. Aupiais, M. Mochizuki, H. Sakata, R. Grasset, Y. Gallais, A. Sacuto, and M. Cazayous, “Colossal electromagnon excitation in the non-cycloidal phase of TbMnO₃ under pressure,” *npj Quantum Mater.* **3**, 60 (2018).

- ¹⁰R. C. Pullar, "Hexagonal ferrites: A review of the synthesis, properties and applications of hexaferrite ceramics," *Prog. Mater. Sci.* **57**, 1191 (2012).
- ¹¹S. Shen, L. Yan, Y. Chai, J. Cong, and Y. Sun, "Magnetic field reversal of electric polarization and magnetoelectric phase diagram of the hexaferrite $Ba_{1.3}Sr_{0.7}Co_{0.9}Zn_{1.1}Fe_{10.8}Al_{1.2}O_{22}$," *Appl. Phys. Lett.* **104**, 032905 (2014).
- ¹²K. Zhai, Y. Wu, S. Shen, W. Tian, H. Cao, Y. Chai, B. C. Chakoumakos, D. Shang, L. Yan, F. Wang, and Y. Sun, "Giant magnetoelectric effects achieved by tuning spin cone symmetry in Y-type hexaferrites," *Nat. Commun.* **8**, 519 (2017).
- ¹³Y. He, D. Hong, N. Su, Y.-S. Chai, Y. Sui, and Y. Sun, "Dynamic magnetoelectric effect of the polar magnet $CaBaCo_4O_7$," *Appl. Phys. Lett.* **126**, 132901 (2025).
- ¹⁴Y. He, Z. Liu, N. Su, D. Hong, and Y. Sun, "Dynamic magnetoelectric effect and phase diagram of the polar magnet Ni_2MnTeO_6 ," *Phys. Rev. B* **112**, 054422 (2025).
- ¹⁵K. Tezuka and Y. Hinatsu, "Magnetic and crystallographic properties of $LnCrO_4$ ($Ln = Nd, Sm, \text{ and } Dy$)," *J. Solid State Chem.* **160**, 362 (2001).
- ¹⁶E. Jiménez, J. Isasi, and R. Sáez-Puche, "Synthesis, structural characterization and magnetic properties of $RCrO_4$ oxides, $R = Nd, Sm, Eu \text{ and } Lu$," *J. Alloys Compd.* **312**, 53 (2000).
- ¹⁷E. Jiménez, J. Isasi, and R. Sáez-Puche, "Field-induced magnetic properties in $RCrO_4$ Oxides ($R = Pr, Gd, Tb, Tm, \text{ and } Yb$)," *J. Solid State Chem.* **164**, 313 (2002).
- ¹⁸E. Climent-Pascual, J. R. d Paz, J. M. Gallardo-Amores, and R. Sáez-Puche, "Ferromagnetism vs antiferromagnetism of the dimorphic $HoCrO_4$ oxide," *Solid State Sci.* **9**, 574 (2007).
- ¹⁹S. Ughade, B. Joshi, and P. Poddar, "Formation of zircon-type $DyCrO_4$ and its magnetic properties," *Ceram. Int.* **48**, 24666 (2022).
- ²⁰X. Wang, I. Loa, K. Syassen, M. Hanfland, and B. Ferrand, "Structural properties of the zircon- and scheelite-type phases of YVO_4 at high pressure," *Phys. Rev. B* **70**, 064109 (2004).
- ²¹Y. W. Long, W. W. Zhang, L. X. Yang, Y. Yu, R. C. Yu, S. Ding, Y. L. Liu, and C. Q. Jin, "Pressure-induced structural phase transition in $CaCrO_4$: Evidence from Raman scattering studies," *Appl. Phys. Lett.* **87**, 181901 (2005).
- ²²Y. W. Long, L. X. Yang, Y. Yu, F. Y. Li, Y. X. Lu, R. C. Yu, Y. L. Liu, and C. Q. Jin, "High-pressure Raman scattering study on zircon- to scheelite-type structural phase transitions of $RCrO_4$," *J. Appl. Phys.* **103**, 15865 (2008).
- ²³Y. Long, Q. Liu, Y. Lv, R. Yu, and C. Jin, "Various $3d-4f$ spin interactions and field-induced metamagnetism in the Cr^{5+} system $DyCrO_4$," *Phys. Rev. B* **83**, 024416 (2011).
- ²⁴X. Shen, L. Zhou, Y. Chai, Y. Wu, Z. Liu, Y. Yin, H. Cao, C. D. Cruz, Y. Sun, C. Jin, A. Munoz, J. A. Alonso, and Y. Long, "Large linear magnetoelectric effect and field-induced ferromagnetism and ferroelectricity in $DyCrO_4$," *NPG Asia Mater.* **11**, 50 (2019).
- ²⁵X. Shen, L. Zhou, Z. Liu, J. He, X. Ye, G. Liu, S. Qin, D. Lu, J. Zhang, Y. Sun, and Y. Long, "Magnetoelectric and magnetostrictive effects in scheelite-type $HoCrO_4$," *Inorg. Chem.* **61**, 14030 (2022).
- ²⁶J. He, Z. Pan, D. Su, X. Shen, J. Zhang, D. Lu, H. Zhao, J. Cong, E. Liu, Y. Long, and Y. Sun, "Magnetic-field-induced sign changes of thermal expansion in $DyCrO_4$," *Chin. Phys. Lett.* **40**, 066501 (2023).
- ²⁷H. Katsura, N. Nagaosa, and A. V. Balatsky, "Spin current and magnetoelectric effect in noncollinear magnets," *Phys. Rev. Lett.* **95**, 057205 (2005).